# Reconstitution of lysosomal NAADP-TRP-ML1 signaling pathway and its function in TRP-ML1 $^{-/-}$ cells

**Fan Zhang, Ming Xu, Wei-Qing Han and Pin-Lan Li**

*Am J Physiol Cell Physiol* 301:C421-C430, 2011. First published 25 May 2011;
doi:10.1152/ajpcell.00393.2010

*Am J Physiol Cell Physiol* 301: C421–C430, 2011.
First published May 25, 2011; doi:10.1152/ajpcell.00393.2010.

# Reconstitution of lysosomal NAADP-TRP-ML1 signaling pathway and its function in TRP-ML1$^{-/-}$ cells

**Fan Zhang, Ming Xu, Wei-Qing Han, and Pin-Lan Li**

*Department of Pharmacology and Toxicology, Medical College of Virginia, Virginia Commonwealth University, Richmond, Virginia*

Submitted 21 September 2010; accepted in final form 17 May 2011

**Zhang F, Xu M, Han WQ, Li PL.** Reconstitution of lysosomal NAADP-TRP-ML1 signaling pathway and its function in TRP-ML1$^{-/-}$ cells. *Am J Physiol Cell Physiol* 301: C421–C430, 2011. First published May 25, 2011; doi:10.1152/ajpcell.00393.2010.—It is well known that the mutation of TRP-ML1 (transient receptor potential-mucolipin-1) causes mucolipidosis IV, a lysosomal storage disease. Given that lysosomal nicotinic acid adenine dinucleotide phosphate (NAADP)-$Ca^{2+}$ release channel activity is associated with TRP-ML1, the present study was designed to test the hypothesis that NAADP regulates lysosome function via activation of TRP-ML1 channel activity. Using lysosomal preparations from wild-type (TRP-ML1$^{+/+}$) human fibroblasts, channel reconstitution experiments demonstrated that NAADP (0.01–1.0 μM) produced a concentration-dependent increase in TRP-ML1 channel activity. This NAADP-induced activation of TRP-ML1 channels could not be observed in lysosomes from TRP-ML1$^{-/-}$ cells, but was restored by introducing a TRP-ML1 transgene into these cells. Microscopic $Ca^{2+}$ fluorescence imaging showed that NAADP significantly increased intracellular $Ca^{2+}$ concentration to 302.4 ± 74.28 nM (vs. 180 ± 44.13 nM of the basal) in TRP-ML1$^{+/+}$ cells, but it had no effect in TRP-ML1$^{-/-}$ cells. If a TRP-ML1 gene was transfected into TRP-ML1$^{-/-}$ cells, the $Ca^{2+}$ response to NAADP was restored to the level comparable to TRP-ML1$^{+/+}$ cells. Functionally, confocal microscopy revealed that NAADP significantly enhanced the dynamic interaction of endosomes and lysosomes and the lipid delivery to lysosomes in TRP-ML1$^{+/+}$ cells. This functional action of NAADP was abolished in TRP-ML1$^{-/-}$ cells, but restored after TRP-ML1 gene was rescued in these cells. Our results suggest that NAADP increases lysosomal TRP-ML1 channel activity to release $Ca^{2+}$, which promotes the interaction of endosomes and lysosomes and thereby regulates lipid transport to lysosomes. Failure of NAADP-TRP-ML1 signaling may be one of the important mechanisms resulting in intracellular lipid trafficking disorder and consequent mucolipidosis.

lysosomes; endosomes; transient receptor potential channels; second messenger; lipid metabolism

THE EFFECTIVE DEGRADATION of lipids by lysosomal acidic hydrolases depends not only on the proper function of these enzymes, but also, importantly, on the timely transport of the endocytosed lipids from endosomes to lysosomes. Obviously, the proper interaction of lysosomes and endosomes plays a critical role in the lipid delivery to lysosomes. Recent studies have demonstrated that the interaction occurs between endosomes and lysosomes in three different modes, namely, vesicular transport (37), kiss and run (33), and hybrid compartments (26, 29). Each mode may produce distinct functions in determining cellular activities. Among them, hybrid compartments are described as a formation of hybrid organelle from endosomes and lysosomes, which, importantly, contributes to the degradation and turnover of macromolecular constituents (24, 26). Clinically, the abnormal lipid trafficking and the defect of interactions between endosomes and lysosomes in the late endocytic pathway may cause mucolipidosis IV, a lysosomal storage disorder, which is characterized by the generalized accumulation of phospholipids, sphingolipids, and acid mucopolysaccharides in lysosomes (3).

On the molecular level, it has been found that the mutation of TRP-ML1 (transient receptor potential-mucolipin 1) is one of critical genetic determinants for the retardation of lysosomal lipid delivery and consequent mucolipidosis (1, 4, 34). It is now known that TRP-ML1 is a nonspecific $Ca^{2+}$-permeable channel, a lysosomal protein with 580-amino acids and six transmembrane-spanning domains. The $NH_2$- and COOH-terminal chains oriented within the cytosol and the ionic pore located between transmembrane segments 5 and 6 (2, 31). The efflux of $Ca^{2+}$ from lysosome compartments through TRP-ML1 channels may play a vital role in the fusion of these organelles and facilitation of subsequent macromolecule metabolism in lysosomes. In our laboratory's recent studies, nicotinic acid adenine dinucleotide phosphate (NAADP) was demonstrated to act on this lysosomal TRP-ML1 channel to induce intracellular $Ca^{2+}$ mobilization in coronary arterial myocytes and hepatocytes (40, 41). Other studies also demonstrated that NAADP could release $Ca^{2+}$ from lysosome-like acidic stores, where the combining mechanism of V-$H^+$-ATPase and $Ca^{2+}/H^+$ exchanger provide a vesicular proton gradients for the sequestration of $Ca^{2+}$ into lysosomal compartments (13, 17). However, it remains unknown whether this NAADP-mediated activation of lysosomal TRP-ML1 channels is functionally implicated in the interaction of lysosomes and endosomes and thereby in the regulation of lipid metabolism of cells.

The present study was designed to test whether NAADP regulates lysosome function via activation of TRP-ML1-$Ca^{2+}$ release channels. Human fibroblasts with TRP-ML1 gene (TRP-ML1$^{+/+}$, wild type) and without TRP-ML1 (TRP-ML1$^{-/-}$) were used to test this hypothesis. In addition, gene rescue experiments were performed to test whether a transgene of TRP-ML1 may restore corresponding lysosomal $Ca^{2+}$ release channel activity and lysosome function. Our results demonstrated that NAADP-induced $Ca^{2+}$ release was abolished when TRP-ML1 gene was deficient in human fibroblasts, and the rescuing of this gene expression restored NAADP-induced $Ca^{2+}$ release and corresponding lysosome function associated with endo-lysosome interactions and lipid delivery to lysosomes.

Address for reprint requests and other correspondence: P.-L. Li, Dept. of Pharmacology and Toxicology, Medical College of Virginia, Virginia Commonwealth Univ., SMB II, Rm 3050, 1220 East Broad St., Richmond, VA 23298 (e-mail: pli@vcu.edu).

## MATERIALS AND METHODS

*Materials.* Human TRP-ML1$^{-/-}$ fibroblast cells were from Coriell Cell Repositories (GM02525), which had been thoroughly studied (4). Wild human fibroblasts were obtained from American Type Culture Collection. Cell cultures were performed with the protocol from the manufacturers. Dextran-conjugated rhodamine and BODIPY-FL C5-lactosylceramide (LacCer) BSA complex were from Molecular Probes. Human green fluorescent protein (GFP)-tagged and untagged TRP-ML1 expression constructs were obtained from OriGene Technologies, TRP-ML1 antibody was from Santa Cruz Biotechnology, (catalog no. sc-48745), and NED-19 was from Enzo Life Science.

*Transfection of TRP-ML1 into TRP-ML1$^{-/-}$ fibroblasts.* The plasmid with confirmed sequence was transfected into TRP-ML1$^{-/-}$ fibroblasts by the TransFectin protocol from Bio-Rad. The transfection efficiency was determined by microscopic detection of the GFP fusion protein at excitation/emission wavelength ($\lambda_{Excitation/Emission}$) of 488/510 nm. The location of the expressed TRP-ML1 was examined by colocalization of GFP-TRP-ML1-associated GFP fusion protein with Alexa Fluor 555-conjugated IgG (A31570, Molecular Probes) plus lysosome-associated membrane protein 1 (Lamp1) primary antibody (ab 25630, Abcam) (Fluor 555/Lamp1) with confocal microscope under $\lambda_{Excitation/Emission}$ (nm) of 488/510 nm and 555/560 nm for GFP and Fluor 555, respectively. The expression of transfected TRP-ML1 in RNA level was tested by iCycler iQ Real-Time PCR Detection System (Bio-Rad) with primers of 5′-ATCGGCATCGAGGCCAAGAA-3′ and 5′-TGTGGAAGAAGGTCAGGTAGCG-3′. Western blot was performed in the purified lysosomal preparations from the gene-transfected cells to further clarify the location of expressed TRP-ML1 by immunoblotting TRP-ML1 $NH_2$-terminal targeted antibody (sc-48745, Santa Cruz Biotechnology).

*Lysosome isolation and identification.* The lysosomes from cultured human fibroblasts were isolated by a lysosome isolation kit (LYSISO1, Sigma) with differential centrifugation, followed by a density gradient centrifugation and $Ca^{2+}$ precipitation, as detailed in the manufacturer's manual. The purity of the prepared lysosomes from fibroblasts was biochemically determined by measuring the activity of acid phosphatase, a lysosomal marker enzyme, with the acid phosphatase assay kit (CS0740, Sigma). The acid phosphatase activity was presented by the conversion of 4-nitrophenyl phosphate to 4-nitrophenol that was measured by spectrophotometer at 405 nm (40, 41). Plasma membrane (PM) and endoplasmic reticulum (ER) components were also prepared from those fibroblasts, with methods described previously (40, 41), and used as controls by analyzing alkaline phosphodiesterase and NADPH-cytochrome *c* reductase for purity of PM and ER preparations, respectively.

*Reconstitution and identification of lysosomal TRP-ML1 channels in lipid bilayer.* The purified lysosomal membranes from human fibroblasts were reconstituted into planar lipid bilayers, as described previously in our laboratory and by others (23, 40, 41, 43). Briefly, phosphatidylethanolamine and phosphatidylserine (1:1) (Avanti Polar Lipids, Alabaster, AL) dissolved in decane (25 mg/ml) were used to form a planar lipid bilayer in a 250-μm aperture between two chambers filled with *cis* and *trans* solutions. After the lipid bilayer was formed, lysosomal membrane preparations (40–60 μg) were added to the *cis* solution. The force of driving lysosomal NAADP channel-containing membranes into the lipid bilayer and promoting their fusion was the electrochemical gradients of $Cs^+$ between the *cis* and *trans* side. In these reconstitution experiments, $Cs^+$ was used as the charge carrier. Axopatch 200B amplifier (Axon Instruments) was applied for the bilayer potential control and currents recording. Data acquisition and analysis were performed with pCLAMP software (version 9, Axon Instruments). The channel open probability ($NP_o$) in the lipid bilayer was determined from 3- to 5-min recordings, and all lipid bilayer experiments were performed at room temperature (~20°C). The lysosomal $Ca^{2+}$ release channel activity was detected in a symmetrical 300 mM cesium methanesulfonate and 10 mM MOPS solution (pH 7.2) with lysosomal preparations from TRP-ML1$^{+/+}$, TRP-ML1$^{-/-}$, or TRP-ML1 gene-rescued TRP-ML1$^{-/-}$ cells.

*NAADP delivery and $Ca^{2+}$ ratiometric measurement.* The NAADP delivery and corresponding $Ca^{2+}$ response determination in different fibroblast cells were performed as our laboratory described previously (43). In brief, fibroblasts were loaded with 10 μM fura-2 at room temperature for 30 min and then washed and buffered in $Ca^{2+}$-free Hanks' solution with 1 mM EGTA. NAADP was mixed and wrapped in Optison reagent with a volume ratio of 1:10 and incubated for 1 min (27, 35, 43), then added to the fura-2-loaded fibroblasts in $Ca^{2+}$- free Hanks' buffer (pH 7.4) for a final concentration of NAADP at 100 nM, followed by ultrasound for 30 s (0.3 W/cm$^2$). Simultaneously, a fluorescence ratio of excitation at 340 nm to that at 380 nm ($F_{340}/F_{380}$) was recorded after background subtraction, and intracellular $Ca^{2+}$ concentration ($[Ca^{2+}]_i$) was calculated by using the following equation: $[Ca^{2+}]_i = K_d\,\beta[(R - R_{min})/(R_{max} - R)]$, where $K_d$ for the fura-2-$Ca^{2+}$ complex is 224 nM; R is the fluorescence ratio ($F_{340}/F_{380}$); $R_{max}$ and $R_{min}$ are the maximal and minimal fluorescence ratios measured by addition of 10 μM of $Ca^{2+}$ ionophore ionomycin to $Ca^{2+}$-replete solution (2.5 mM $CaCl_2$) and $Ca^{2+}$-free solution (5 mM EGTA), respectively; and β is the fluorescence ratio at 380-nm excitation determined at $R_{min}$ and $R_{max}$, respectively (16, 38). The untreated fibroblasts were also applied to ultrasound microbubble treatment for each group as a control. Several groups of fibroblasts were pretreated with 100 nM bafilomycin (a lysosome function inhibitor), 0.5 mM glycylphenylalanine 2-naphthylamide (a lysosome disruptor), 50 μM pyridoxal-phosphate-6-azophenyl-2′,4′-disulfonic acid (PPADS) or 10 μM NED-19 (26a) (two NAADP antagonists), 100 nM 2-aminoethoxydiphenyl borate (an inositol 1,4,5-trisphosphate antagonist) or 50 μM ryanodine (Rya; a ryanodine receptor blocker) for 15 min, followed by NAADP delivery and $Ca^{2+}$ release ratiometric determination.

*Confocal microscopic analysis of endosome and lysosome dynamic interactions.* Human fibroblasts were incubated with dextran-conjugated rhodamine (0.4 mg/ml) for 4 h in color-free M199 cell culture medium containing 10% FBS at 37°C, 5% $CO_2$, followed by a 24-h chase in rhodamine-free medium (9). These rhodamine-loaded fibroblasts were subsequently incubated with Oregon green 488 (0.5 mg/ml) for 10 min and then treated with vehicle, or PPADS (50 μM), and incubated for another 10 min. In another group experiment, rhodamine- and Oregon green 488-loaded wild and TRP-ML1-rescued fibroblasts were bathed in $Ca^{2+}$-free Hanks' solution with 10 μM BAPTA-AM (6), a cell-permeable intracellular calcium chelator, to determine the effects of elimination of the released $Ca^{2+}$ by TRP-ML1 on lysosome-endosome interaction. The confocal fluorescent microscopic recording was conducted with an Olympus Fluoview System, which consists of an Olympus BX61WI inverted microscope with an Olympus Lumplan F1×60, 0.9 numerical aperture, and water-immersion objective (42). For NAADP treatment, immediately before transferring to confocal microscopic stage, NAADP was delivered into the cells at a concentration of 100 nM, as described above. The fluorescence images of the cells were dynamically recorded at $\lambda_{Excitation/Emission}$ of 568/590 and 488/530 nm for lysosomes (rhodamine red) and endosomes (Oregon green) by XYT recording mode with a speed of 1 frame/s, as described previously (42). The interaction of lysosomes and endosomes was presented by the generation of yellow spots, and the corresponding intensity was analyzed by Image Pro-Plus software. Under the count/size measurement mode, the yellow spot was defined by using color tube-based tool, and the configuration of these yellow color parameters was applied to the subsequent serial image analysis. In a single experiment, five cells were randomly chosen, the individual whole cell yellow spot intensity was measured, and the average value from these five cells was taken, which was normalized to the lysosome fluorescence (rhodamine red) intensity in the related image for data analysis of results.

*Confocal microscopic analysis of BODIPY-LacCer delivery to lysosomes.* Human fibroblasts were first incubated with Dextran-conjugated rhodamine (0.4 mg/ml) for lysosomal labeling, as described above. These rhodamine-loaded fibroblasts were subsequently incubated with DMEM medium containing 5 μM BODIPY-FL C5-LacCer BSA complex at 37°C, 5% $CO_2$, for 15 min (12). After wash with PBS, the PM bounded LacCer was back exchanged with ice-cold DMEM containing 5% fatty acid-free BSA at 4°C (3 × 15 min). Endocytosed LacCer was then chased for 24 h to allow lipid transport from endosomes to lysosomes. To investigate the role of NAADP/TRP-ML1 signaling pathway in the lipid endocytic trafficking, the NAADP antagonists of PPADS (50 μM) or NED-19 (10 μM) and lysosome function inhibitor of bafilomycin A1 (100 nM), as well as NAADP (100 nM), were applied to the cells immediately before chasing, as described above. At the end of chase point, the cells were fixed in the ice-cold 4% formaldehyde, and digital confocal fluorescent microscopic images were obtained through the Olympus Fluoview System at $\lambda_{Excitation/Emission}$ of 568/590 and 488/530 nm for lysosomes (rhodamine) and endosomes (LacCer), respectively. The yellow spots in the merged image represent the delivery of LacCer from endosomes to lysosomes. The colocalization coefficiency from the whole cell area was quantified by the Image Pro-Plus software. Under the co-colocalization measurement, the red and green color pair was applied for the colocalization coefficient analysis. In a single experiment, five cells were randomly chosen, and the averaged value was taken for statistics.

*Statistics.* Data are presented as means ± SE. Significant differences between and within multiple groups were examined using ANOVA for repeated measures, followed by Duncan's multiple-range test. Student's *t*-test was used to evaluate the significant differences between two groups of observations. $P < 0.05$ was considered statistically significant.

## RESULTS

*Confirmation of the purified lysosomes.* The purity of lysosomes was confirmed by the biochemical measurement of the specific marker enzyme activity among the isolated cell components. As shown in Fig. 1, the conversion rate of 4-nitrophenyl phosphate to 4-nitrophenyl by lysosome marker enzyme, acid phosphatase, was 1.08 ± 0.26, 10.57 ± 1.94, 0.48 ± 0.29, and 0.73 ± 0.32 $\mu mol \cdot h^{-1} \cdot mg^{-1}$ protein in the preparations of cell homogenate, lysosome, ER, and cell PM, respectively, with the highest enzymatic activity in lysosomal preparation. However, the ER marker enzyme of NADPH-cytochrome *c* reductase was only markedly detected in the isolated ER component, but modest in lysosomal preparations. Similarly, the significant alkaline phosphodiesterase activity was only found in PM components, but not in other preparations, including lysosomes. These results indicate that the isolated lysosomes are highly purified and free of ER and cell membrane contamination. Such highly purified lysosomal preparations were applied in the channel reconstitution studies.

*Expression and localization of transfected TRP-ML1 construct.* To clarify the role of TRP-ML1 in mediating NAADP-induced $Ca^{2+}$ release from lysosomes and its functional significance in lipid endocytic trafficking, the gene rescue was performed in TRP-ML1$^{-/-}$ fibroblasts with full length of human TRP-ML1. As shown in Fig. 2*A*, the immunocytochemistry results from confocal microscopy of a single in-depth section image of the transfected cells demonstrated that the expressed fusion protein of GFP-TRP-ML1 (green) was colocalized well with Lamp1-conjugated Fluor 555 (red) and the yellow spots generated in the merged image. However, few yellow spots were found in the GFP control group (TRP-ML1$^{-/-}$ fibroblasts transfected with GFP only). In RNA level, real-time PCR results demonstrated that the expression of TRP-ML1 was significantly increased compared with the GFP control group (Fig. 2*B*), and the immunoblotting documents further revealed that TRP-ML1 transfection cells had markedly enhanced TRP-ML1-intact protein in lysosomal preparation compared with control. The genetic background of functional deficiency TRP-ML1$^{-/-}$ fibroblasts used in the presented study had been well exploited (4). It was found that this TRP-ML1 defect cell had a deletion of 6,432 bp in genomic DNA, which corresponds to the first 5 extrons and partial 6th extron out of a total 13 extrons from the 5′ end in intact TRP-ML1 gene. Both of the primers used in the mRNA analysis and the antibody for TRP-ML1 protein detection are within the retained TRP-ML1 fragments. The detected mRNA and cleaved TRP-ML1 protein in the control group are attributed to the remnant presence of nonfunctional and mutated TRP-ML1.

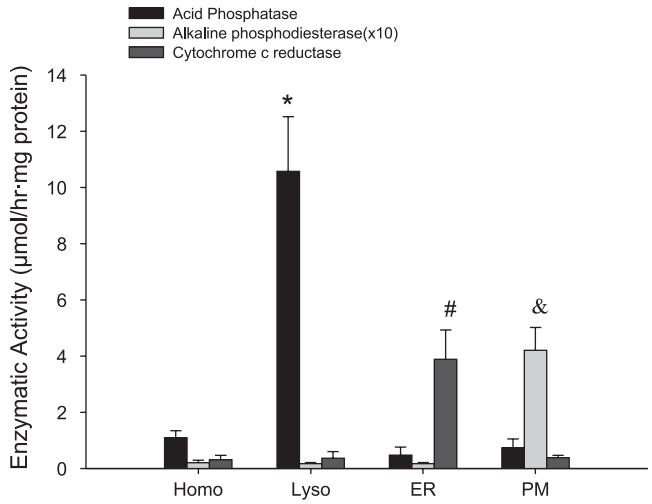


Fig. 1. Enzymatic confirmation of the purity of lysosome (Lyso) preparation. The Lyso marker enzyme of acid phosphatase has the highest activity in lysosomal preparation among the isolated cell components of Lyso, endoplasmic reticulum (ER), plasma membrane (PM), and cell homogenates (Homo), whereas PM marker enzyme of alkaline phosphodiesterase and ER marker enzyme of NADPH-cytochrome *c* reductase were barely detected in lysosomal preparation, but were only found abundant in the correspondingly represented components. Values are means ± SE. $P < 0.05$: *Lyso, #ER, and & PM significantly different from corresponding enzymatic activity in other group ($n = 6$ batches of preparations).

These results suggest that the transfected intact TRP-ML1 was highly expressed in the lysosomes and would salvage TRP-ML1 function in the mutated cells. The transfection of untagged TRP-ML1 in fibroblasts was used in the subsequent gene rescue studies.

*Concentration-dependent effects of NAADP on reconstituted lysosomal channel activity.* Since the lysosomes are not accessible by conventional patch-clamp method, lipid bilayer reconstitution of lysosomal channels was used to investigate their properties. A concentration-dependent response of these reconstituted channels to NAADP was first tested. Figure 3*A* depicts representative recordings of single-channel $Cs^+$ currents before and after application of different concentrations of NAADP into the *cis* solution at a holding potential of +40 mV. It was shown that NAADP at 0.01–1.0 μM significantly increased the openings of this reconstituted lysosomal channel

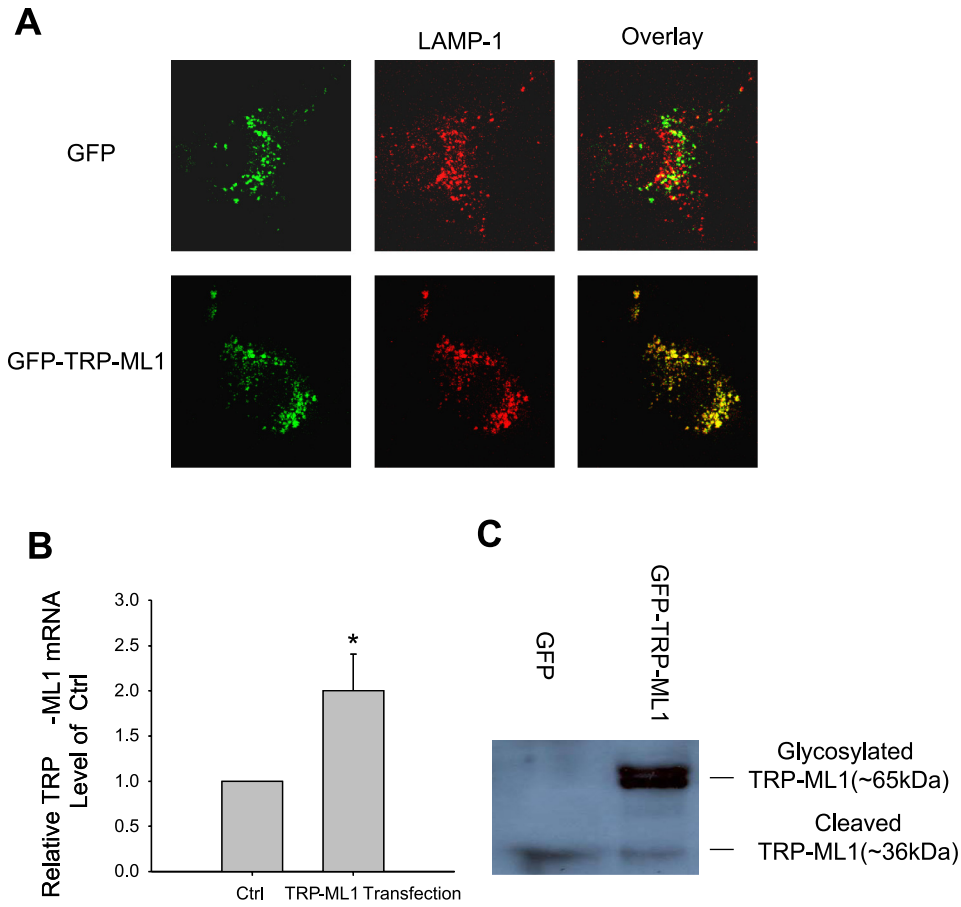


Fig. 2. Confirmation of the location of transfected transient receptor potential-mucolipin-1 (TRP-ML1) on Lyso in TRP-ML1 deficiency fibroblasts. *A*: representative confocal microscopic images show that the expressed fusion protein of green fluorescent protein (GFP)-TRP-ML1 (green) is colocalized well with Lyso-associated membrane protein 1 (Lamp1)-conjugated Fluor 555 (red) and the yellow spots generated in the merged image. However, few yellow spots are found in the GFP control (Ctrl) group (TRP-ML1$^{-/-}$ fibroblasts transfected with GFP only). *B*: real-time PCR results demonstrate that the expression of TRP-ML1 RNA was significantly increased after TRP-ML1 transfection. *$P < 0.05$, significant difference from control group ($n = 3$~4). *C*: the immunoblotting results indicate that expressed TRP-ML1 protein was markedly enhanced in lysosomal preparation.

from TRP-ML1$^{+/+}$ cells. However, NAADP at 100 μM could not produce more increase in channel activity compared with that at 1 μM. Figure 3*B* summarized the results, showing the effect of NAADP on the $NP_O$ of this reconstituted $Ca^{2+}$ release channel. NAADP increased lysosomal $Ca^{2+}$ release channel $NP_o$ from 0.00812 ± 0.00213 of the basal level to 0.0926 ± 0.0170 at 1 μM NAADP, but decreased to 0.0383 ± 0.00526 after 100 μM NAADP was applied. This bell-shaped effect of NAADP at different concentrations represents a typical NAADP-sensitive $Ca^{2+}$ release channel in such preparations.

To further characterize this channel in human fibroblasts, some pharmacological interventions to identify TRP-ML1 channels were used, as in our previous studies in liver and smooth muscle cells (40, 41). As shown in Fig. 4*A*, in lysosomal preparations from wild-type fibroblasts, L-type $Ca^{2+}$ channel antagonists, nifedipine (100 μM) or verapamil (100 μM), and $Na^+$ channel blocker of amiloride (100 μM), which are commonly used to characterize TRP-ML1 channels, all significantly attenuated NAADP-induced increase in lysosomal $Ca^{2+}$ release channel $NP_O$. Similarly, PPADS (50 μM) and NED-19 (10 μM), two NAADP antagonists, also significantly decreased the response of this lysosomal channel to NAADP. As a negative control, cADP ribose (100 nM) had no effects on the $NP_o$ of this channel. These pharmacological properties indicate that this NAADP-activated lysosomal channel is a nonselective $Ca^{2+}$ channel with characteristics of TRP-ML1. However, this lysosomal NAADP-sensitive $Ca^{2+}$ channel activity could not be observed in lysosomal preparations from TRP-ML1$^{-/-}$ fibroblasts. Furthermore, when these TRP-ML1$^{-/-}$ cells were introduced as a recombinant human TRP-ML1 gene, the channel activity was restored to the level comparable to that observed in TRP-ML1$^{+/+}$ cells (Fig. 4*B*). These results further confirmed that TRP-ML1 is an NAADP-sensitive $Ca^{2+}$ release channel in lysosomes.

*Fluorescence imaging analysis of $Ca^{2+}$ release by NAADP.* Given that NAADP could activate lysosomal TRP-ML1 channels in lipid bilayer reconstitution, we further analyzed NAADP-induced $Ca^{2+}$ release response in intact fibroblast with different TRP-ML1 genetic background using fluorescent imaging techniques. Figure 5*A* was the real-time $Ca^{2+}$ release trace in response to the NAADP stimulation, which indicates the immediate $Ca^{2+}$ responses after NAADP delivery. Summarized results in Fig. 5*B* showed that NAADP significantly enhanced $Ca^{2+}$ release from TRP-ML1$^{+/+}$ fibroblasts (180 ± 44.13 of control to 302.4 ± 74.28 of NAADP). Lysosomal function inhibitors, bafilomycin A1 and glycylphenylalanine 2-naphthylamide, and NAADP antagonists of PPADS and NED-19 significantly attenuated NAADP-induced $Ca^{2+}$ release in these cells. However, ER-$Ca^{2+}$ channel antagonists, Rya (50 μM) and inositol 1,4,5-trisphosphate/$Ca^{2+}$ channel blocker, 2-aminoethoxydiphenyl borate, had no effects on NAADP-induced $Ca^{2+}$ responses. Moreover, this NAADP-induced $Ca^{2+}$ release response could not be observed in TRP-ML1$^{-/-}$ fibroblasts. With introduction of TRP-ML1 gene into TRP-ML1$^{-/-}$ cells, the NAADP-induced $Ca^{2+}$ response was recovered (Fig. 5*C*).

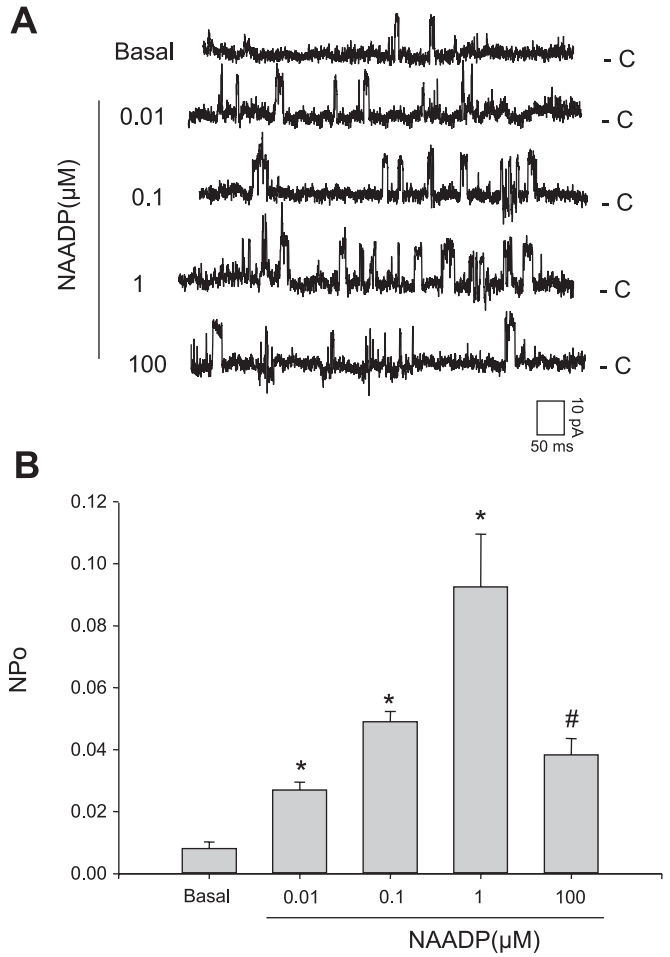


Fig. 3. Concentration-dependent responses of nicotinic acid adenine dinucleotide phosphate (NAADP) on the reconstituted lysosomal $Ca^{2+}$ release channel activity by lipid bilayer assay. *A*: representative recording of NAADP-sensitive $Ca^{2+}$ channel currents at different concentrations of NAADP at holding potential +40 mV. *B*: summarized $NP_o$ (open-channel probability) when lysosomal preparation from wild-type human fibroblast cells is treated with NAADP from 0.01 to 100 μM. Values are means ± SE. $*P < 0.05$, significant difference from basal level. $\#P < 0.05$ vs. 1 μM group ($n = 6$).

*NAADP-stimulated interactions of endosomes and lysosomes in human fibroblasts by confocal microscopic assay.* Since lysosomal TRP-ML1 $Ca^{2+}$ release channels were sensitive to NAADP, and lack of TRP-ML1 could cause aberrant lipid endocytotic trafficking, we wondered whether NAADP may regulate lipid endocytosis due to influence on delivery of lipids to lysosomes. Figure 6 showed dynamic interactions of endosomes and lysosomes recorded by confocal microscopy in fibroblasts with different TRP-ML1 background. Confocal image with maximal yellow spots in 10-min dynamic recording is presented in Fig. 6*A*. Dextran-conjugated rhodamine red represented lysosomes, and Oregon green fluorescence indicated endosomes. Yellow spots in these images displayed the mixed content between endosomes and lysosomes. In TRP-$ML1^{-/-}$ cells, the relative positions of endosomes and lysosomes had no obvious change during the 10-min recording, and very few yellow spots were observed. In TRP-$ML1^{+/+}$ cells, however, the interaction of endosomes and lysosomes was detected, and yellow spots were markedly increased. When TRP-$ML1^{+/+}$ cells were stimulated with NAADP, yellow spots and corresponding intensity were further enhanced (a short movie is presented in electronic supplemental materials for dynamic interaction of lysosomes and endosomes; the online version of this article contains supplemental data) (other group images not shown). Figure 6*B* summarized the results from these experiments. Among different groups, cells with TRP-$ML1^{+/+}$ and TRP-$ML1^{-/-}$ plus a transgene show strong interaction of lysosomes and endosomes (yellow spots generation). NAADP enhanced the interactions in these cells, which was blockable by its antagonist, PPADS. Similarly, in wild type or TRP-$ML^{-/-}$, with TRP-ML1 gene rescued cells

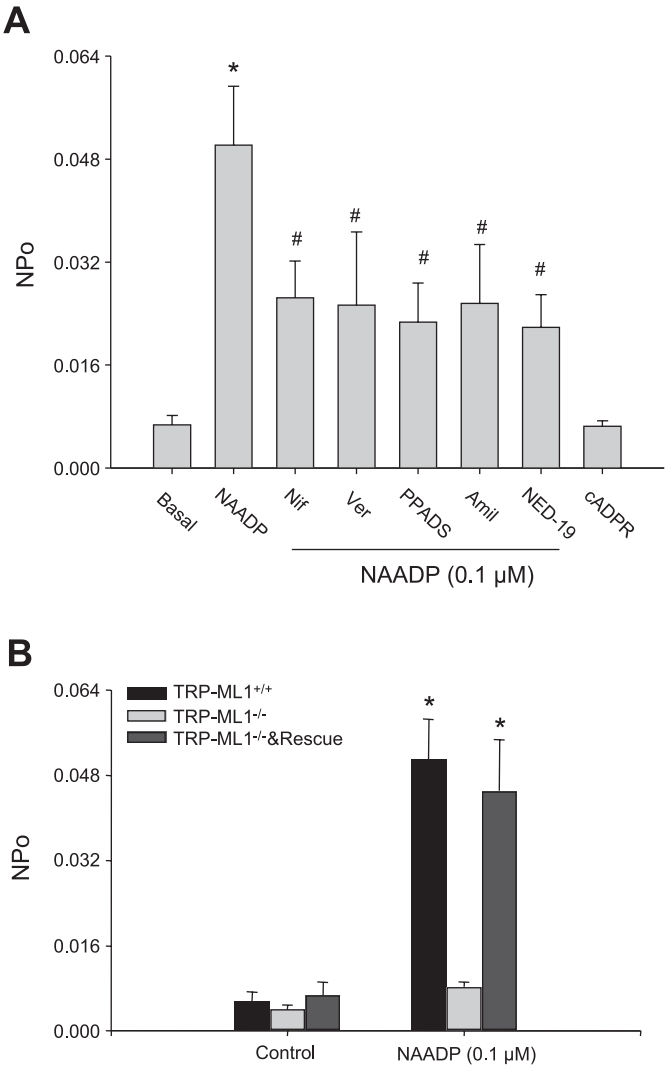


Fig. 4. Identification of lysosomal NAADP-sensitive $Ca^{2+}$ release channels as TRP-ML1 function by lipid bilayer assay. *A*: summarized NAADP-TRP-ML1 $NP_o$ in Lyso preparation from wild-type fibroblasts under control condition and by treatment of bilayer with 0.1 μM NAADP before and after addition of nifidipine (Nif; 100 μM), verapamil (Ver; 100 μM), pyridoxal-phosphate-6-azophenyl-2′,4′-disulfonic acid (PPADS; 50 μM), NED-19 (10 μM), or amiloride (Amil; 100 μM), and cADP ribose (cADPR) was used as negative control. *B*: summarized TRP-ML1 $NP_o$ results show that lysosomal preparation with TRP-ML1 deficiency (TRP-$ML1^{-/-}$) has no $Ca^{2+}$ release effects on NAADP (0.1 μM) stimulation. However, when rescued by TRP-ML1 transfection (TRP-$ML1^{-/-}$ & Rescue), the lysosomal $Ca^{2+}$ channel response to NAADP is recovered to that in wild-type cell level (TRP-$ML1^{+/+}$). Values are means ± SE. $*P < 0.05$, significant difference from TRP-$ML1^{-/-}$ group or basal. $\#P < 0.05$, compared with NAADP-alone group ($n = 6$).

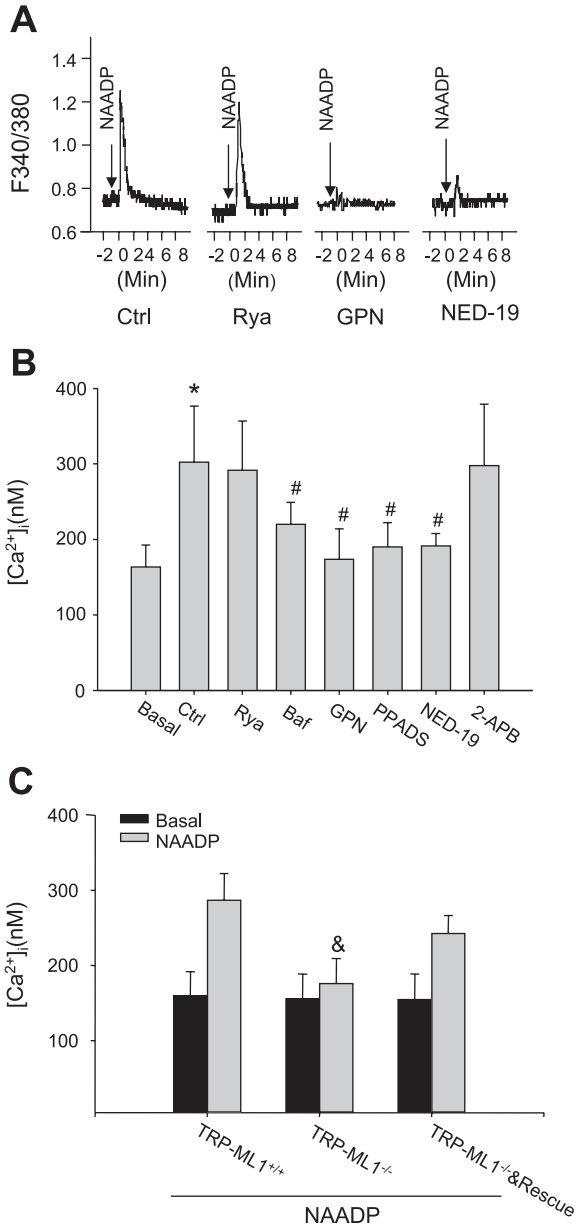


Fig. 5. NAADP-induced $Ca^{2+}$ release response by fluorescence image $Ca^{2+}$ analysis. *A*: the real-time $Ca^{2+}$ release trace in response to the NAADP stimulation. *B*: summarized results show the effects of different antagonists on NAADP-induced $Ca^{2+}$ release in TRP-ML1$^{+/+}$ fibroblast cells. *C*: in TRP-ML1 deficiency (TRP-ML1$^{-/-}$) human fibroblast cells, NAADP-induced $Ca^{2+}$ release was almost completely deprived. However, when rescued with TRP-ML1 (TRP-ML1$^{-/-}$ & Rescue), this $Ca^{2+}$ response was recovered to that in TRP-ML1 wild-type (TRP-ML1$^{+/+}$) level. Values are means ± SE. F340/380, fluorescence ratio of excitation at 340 nm to that at 380 nm; $[Ca^{2+}]_i$, intracellular $Ca^{2+}$ concentration; Rya, ryanodine; Baf, bafilomycin; GPN, glycylphenylalanine 2-naphthylamide; 2-APB, 2-aminoethoxydiphenyl borate. *$P < 0.05$ vs. basal level. #$P < 0.05$ vs. NAADP-only group. & $P < 0.05$ vs. TRP-ML1$^{+/+}$ group or TRP-ML1$^{-/-}$ &Rescue group ($n = 6$).

treated with BAPTA-AM, a cell-permeable $Ca^{2+}$ chelator, stimulation of TRP-ML1 by NAADP no longer produced an enhanced interaction between endosomes and lysosomes. In TRP-ML1$^{-/-}$ cells, such interaction of lysosomes and endosomes, as well as NAADP-induced enhancement, also could not be observed.

*Functional role of NAADP/TRP-ML1 signaling in the promotion of lipids endocytic trafficking.* Since NAADP/TRP-ML1 signaling contributed to the regulation of endosome and lysosome interaction, we wonder if this pathway may play a critical role in the regulation of lipids delivery from endosomes to lysosomes. In the wild type of fibroblasts with treatment of NAADP, the endocytosed LacCer in endosomes (green) was found to be increasingly chased to and colocalized well with lysosomes to generate yellow spots in the merged image (NAADP panel in Fig. 7*A*) compared with vehicle group. However, when the cells were pretreated with lysosomal inhibitor, bafilomycin A1, or NAADP antagonists, PPADS and NED-19, the ability of NAADP to drive LacCer to lysosomes

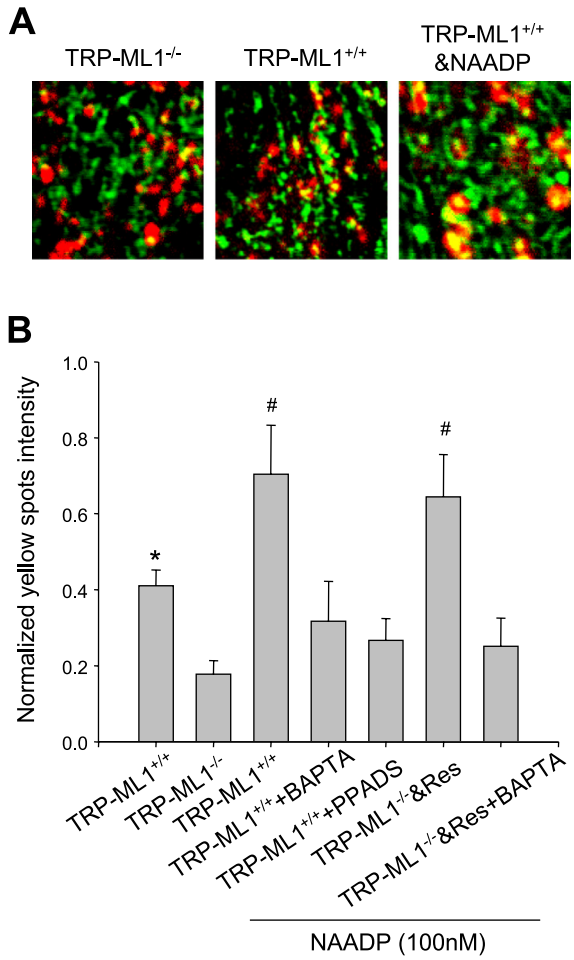


Fig. 6. NAADP/TRP-ML1-dependent interaction of endosomes (Endo) and Lyso in human fibroblast cells by confocal microscopic assay. *A*: dextran-conjugated rhodamine (Rho) red shows the trace of Lyso, Oregon green 488 indicates the Endo, and the yellow spots demonstrate the mixed content between Endo and Lyso. In TRP-ML1$^{-/-}$ group, the relative positions of Endo and Lyso have no obvious change during the 10-min recording; consistently, there are few yellow spots observed. However, in TRP-ML1$^{+/+}$ panel, the interaction of Endo and Lyso is significantly increased, and the yellow spot intensity was subsequently enhanced. When TRP-ML1$^{+/+}$ is treated with NAADP, the yellow spot intensity was further elevated. *B*: the summary of normalized yellow spot density among different groups in 10-min image recording, which indicates that the presence of TRP-ML1 could increase the Endo and Lyso interaction and result in a significant increase of yellow intensity compared with that of TRP-ML1 deficiency cells, and NAADP could further enhance the process. Res, rescue. Values are means ± SE. *$P < 0.05$ vs. TRP-ML1$^{-/-}$ group. #$P < 0.05$ vs. TRP-ML1$^{+/+}$-only group ($n = 5$~6).

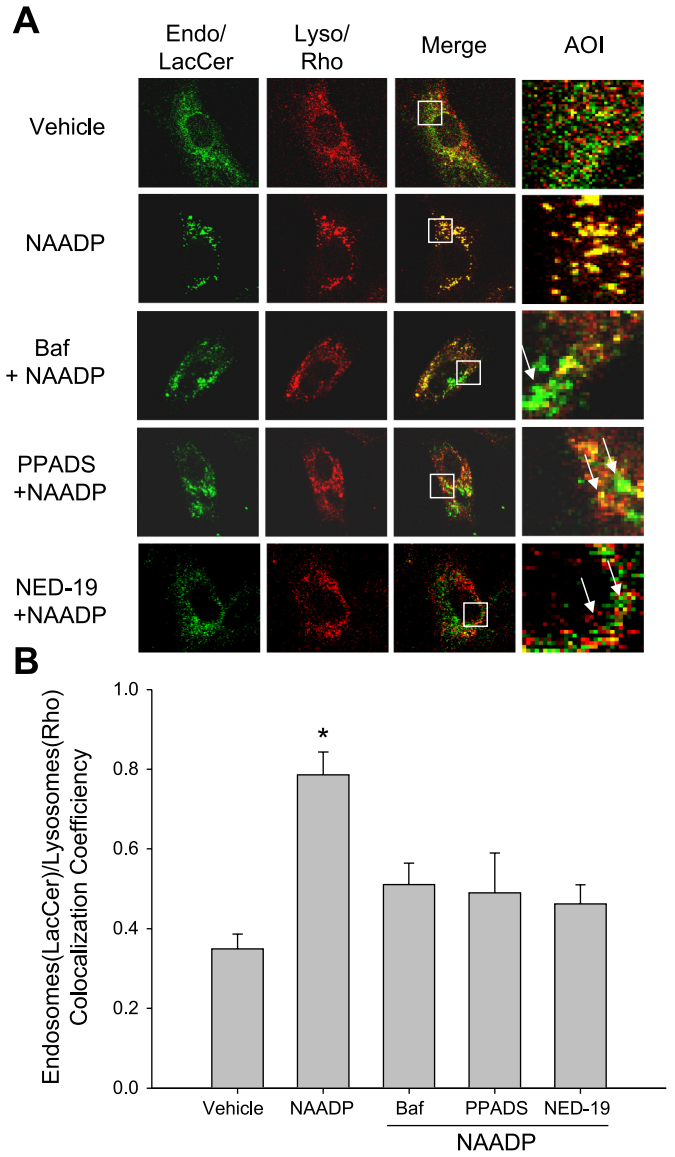


Fig. 7. Activation of NAADP/TRP-ML1 signaling promotes the endocytosed lactosylceramide (LacCer) trafficking to Lyso in wild-type fibroblasts. *A*: confocal images show endocytosed LacCer (Endo, green), Rho-loaded Lyso (red), and the colocalization of Endo and Lyso (yellow) among different groups. AOI (area of interest) is the amplified square area from overlay image. Arrows indicate the enlargement of Endo or Endo-Lyso hybrids. *B*: summarized colocalization coefficiency between LacCer-filled Endo and Rho-loaded Lyso among different groups. Values are means ± SE. *$P < 0.05$ vs. other groups ($n = 5$~6).

was significantly attenuated; instead, the LacCer-occupied endosome compartment was enlarged, as seen (arrow indicated) in the area of interest panel from the amplified square region. Consequently, the colocalization of endosomes/LacCer and lysosomes/rhodamine was decreased. Figure 7*B* summarized the colocalization coefficiency between LacCer-filled endosomes and rhodamine-loaded lysosomes among different groups, with the highest in the NAADP group. In bafilomycin A1-, PPADS-, and NED-19-treated groups, there was no significant increase in colocalization coefficiency compared with NAADP group.

In TRP-ML1$^{-/-}$ fibroblasts, NAADP had no enhancement effects on the delivery of endocytosed LacCer to lysosomes, with only a few yellow spots generated in the merged image similar to that in the vehicle group (Fig. 8*A*). However, the accumulation of LacCer in endosomes was detected as that observed in the wild type of cells by blocking NAADP/TRP-ML1 pathway, which resulted in the endosome compartment enlargement (area of interest panel in both NAADP and vehicle groups, arrow indicated). After TRP-ML1 gene rescue, the delivery of endocytosed LacCer from endosomes to lysosomes was restored to the level in wild-type cells, and significant colocalization was observed in the merged image (yellow spots in TRP-ML1 and NAADP panel). Figure 8*B* is the summarized results. The colocalization coefficiency between endosomes and lysosomes was markedly higher in the TRP-ML1 and rescue plus NAADP group compared with NAADP-only or vehicle group.

## DISCUSSION

The present study demonstrated that TRP-ML1 functions as an NAADP-sensitive $Ca^{2+}$ release channel to release $Ca^{2+}$ from lysosomes in human fibroblasts, and NAADP/TRP-ML1 signaling functionally promotes the interaction of endosomes and lysosomes and the lipid endocytic delivery to lysosomes.

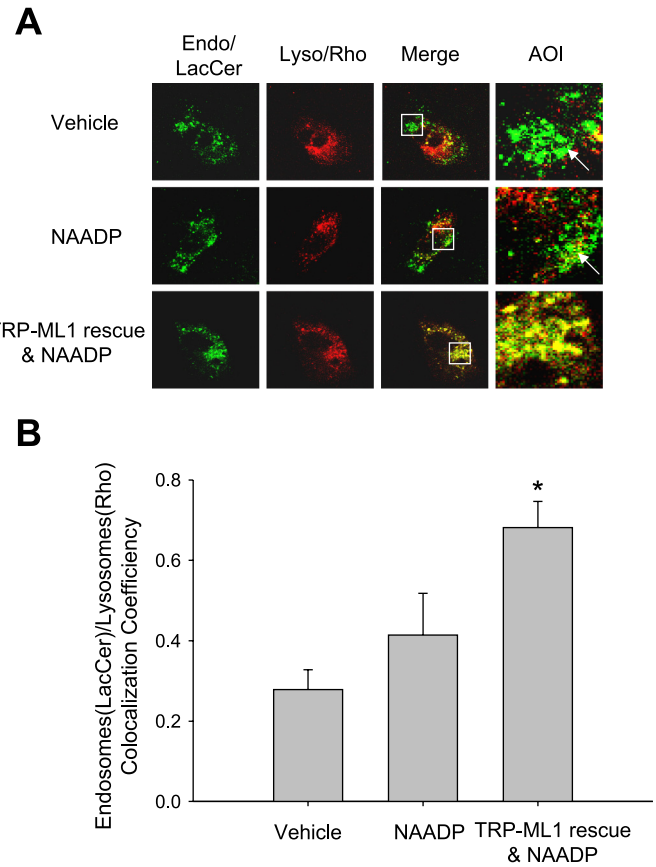


Fig. 8. Rescuing TRP-ML1 expression in TRP-ML1$^{-/-}$ fibroblasts restores the NAADP/TRP-ML1 signaling in the delivery of endocytosed LacCer to Lyso. *A*: representative confocal images show the transportation of LacCer to Lyso in TRP-ML1$^{-/-}$ and TRP-ML1 rescued cells. Yellow spots in merged images indicate the delivery of LacCer (green) to Lyso (red). AOI is the amplified square area from overlay image. Arrows indicate the enlargement of Endo or Endo-Lyso hybrids. *B*: summarized colocalization coefficiency between LacCer-filled Endo and Rho-loaded Lyso among different groups. Values are means ± SE. *$P < 0.05$ vs. other groups ($n = 5$).

Since NAADP was first identified as the most potent intracellular $Ca^{2+}$ mobilizer in sea urchin egg homogenates a decade ago (22), the nature of NAADP-targeted $Ca^{2+}$ store and targeted intracellular channels is still controversial. Currently, both lysosomes-like acidic compartments and ER have been suggested as the target organelles for NAADP to release $Ca^{2+}$, depending on cell types studied (14, 32). By lysosomal channel reconstitution, our laboratory recently reported that NAADP may act on TRP-ML1 to induce lysosome-associated $Ca^{2+}$ release in liver cells and vascular smooth muscle cells (40, 41). In the present study, we used purified lysosomes prepared from TRP-ML1-deficient human fibroblasts and further confirmed that an NAADP-sensitive $Ca^{2+}$ channel is associated with TRP-ML1. Our results demonstrated that there was no NAADP-stimulated channel activity in lysosomes from TRP-ML1$^{-/-}$ cells. However, when a human TRP-ML1 gene was introduced into these TRP-ML1-deficient cells, the NAADP-induced lysosomal channel activity and $Ca^{2+}$ release response were restored. Biophysically and pharmacologically, this NAADP-sensitive channel was also similar to TRP-ML1. Based on these results, we conclude that lysosomal TRP-ML1 may mediate the activity of an NAADP-sensitive channel, which may be responsible for lysosome $Ca^{2+}$ release induced by NAADP and thereby regulate a variety of lysosome functions.

With respect to the targets of NAADP, it has recently been reported that some other ion channels can be candidates, such as Rya/$Ca^{2+}$ receptor in jurkat T-lymphocytes (21), transient receptor potential member 2 in neutrophil (20) and jurkat T-lymphocytes (5), and $P2Y_{11}$ purinergic receptors in transfected astrocytoma cells (25). Most recently, two-pore channels (TPCs; TPC1, TPC2, and TPC3) were reported as NAADP-sensitive $Ca^{2+}$-permeable channels (7, 8, 10, 44). With overexpression study, all of these TPCs, despite profound diversity in sequence, were found to potentate NAADP-medicated calcium signals in lysosome-like acidic organelles. Obviously, direct evidence from recording such NAADP-activated TPC channel in lysosomes from native tissue is needed. Given the variety of NAADP channel identity in different types of cells, it is possible that these targets of NAADP may be tissue specific in the regulation of corresponding cell functions, or a common accessory NAADP binding protein exists, which facilitates NAADP-associated $Ca^{2+}$ release. It also should be noted that the major location of reported TPCs in mediation of $Ca^{2+}$ release by NAADP was on lysosome-like intracellular acidic vesicles (7, 10), but not in lysosomes, where TRP-ML1 has been identified as the NAADP-sensitive $Ca^{2+}$ channel (40, 41), similar to the findings of the present study. Therefore, the location difference of NAADP-sensitive $Ca^{2+}$ channel may contribute to the different channel identity in mediation of $Ca^{2+}$ release by NAADP as well.

Another important finding of the present study is that NAADP regulates lysosomal function through activation of lysosomal TRP-ML1. In the endosome and lysosome interaction study that was performed among cell groups of TRP-ML1$^{-/-}$, TRP-ML1$^{+/+}$, and TRP-ML1$^{+/+}$ plus NAADP, the TRP-ML1$^{-/-}$ group of cells had the modest yellow spots formed by lysosome- and endosome-specific dye staining. Cells of TRP-ML1$^{+/+}$ plus NAADP stimulation exhibited the highest yellow spot intensity. These results suggest that fusion of endosomes and lysosomes is dependent on the intact function of TRP-ML1, and that NAADP promotes this dynamic process. Since TRP-ML1 acts as a lysosomal NAADP-sensitive $Ca^{2+}$ channel and NAADP could induce TRP-ML1-associated $Ca^{2+}$ release from lysosomes, enhancement of endosome and lysosome interaction may be attributed to the TRP-ML1-mediated $Ca^{2+}$ release from lysosomes. In this regard, it has been found that both microtubules and actin filaments are involved in the regulation of membrane dynamics along the endocytic pathway (15, 19), and a large number of actin-based mechanoenzymes, related to muscle myosin and to brush board myosin I, have been identified (19). The local generated $Ca^{2+}$ from lysosomes by NAADP may act to bind and modulate essential components of the endosomal transport machinery and facilitate endosome trafficking to lysosomes. However, the precise mechanism remains to be defined.

The interactions between endosomes and lysosomes by "kiss and run" and "hybrid compartments" formation are responsible for the endocytic delivery of materials to lysosomes. In this regard, previous studies from a cell-free system in yeast have shown that luminal $Ca^{2+}$ release induced homotypic vacuole fusion (28). Moreover, this $Ca^{2+}$-dependent homotypic fusion of early endosomes and heterotypic fusion of late endosomes with lysosomes was also observed in the subcellular fractions from mammalian cells (18, 29). To test the function implication of NAADP-activated TRP-ML1 in lipid delivery, we applied a fluorescent conjugate of BODIPY-C5-LacCer BSA, a popular green fluorescent analog that has been used for screening this TRP-ML1-associated lipid storage disorder in lysosomes (12), and found that NAADP had no enhancement effects on the delivery of endocytosed LacCer to lysosomes in TRP-ML1$^{-/-}$ fibroblasts. Furthermore, the accumulation of LacCer in endosomes was detected in TRP-ML1$^{-/-}$ cells and in the wild type of cells by blocking NAADP/TRP-ML1 pathway, which resulted in the endosomal compartment enlargement. These findings are consistent with previous observations that TRP-ML1-deficient cells exhibit an aberrant mixing of endosomal and lysosomal content (11) and swollen endosomal/lysosomal compartments as well (36). Interestingly, we also found that bafilomycin A1, a common inhibitor of lysosome function, had inhibitory effects on LacCer endocytic trafficking to lysosomes as the TRP-ML1 antagonists do. V-$H^+$-ATPase is a lysosome-resident proton pump that actively maintains an acidic milieu in the lysosomal lumen, which acts to drive $Ca^{2+}$ uptake into the lysosomes by $Ca^{2+}/H^+$ exchange. Therefore, inhibition of V-$H^+$-ATPase may cause the depletion of $Ca^{2+}$ storage in lysosomes and led to no $Ca^{2+}$ release response through TRP-ML1 on NAADP stimulation. This evidence further supports the fact that the $Ca^{2+}$ release from TRP-ML1 channels is critical in the regulation of lipid internal delivery to lysosomes. The quick delivery of macromolecules from endosomes to lysosomes may contribute to higher lipid metabolism rate in lysosomes. In the context, abnormal endocytosis processes of membrane components from late endosomes to the lysosomes and/or delayed efflux to the Golgi apparatus were identified as an important pathological change in heterogeneous storage disorders in mucolipidosis type IV patients. The rescue of the mutated TRP-ML1 by transecting of wild-type TRP-ML1 was found to correct such aberrant LacCer trafficking in mucolipidosis type IV cells (30).

In summary, the present study demonstrated that lysosomal TRP-ML1 functions as the NAADP-sensitive $Ca^{2+}$ release channel in human fibroblasts. NAADP-induced activation of lysosomal TRP-ML1 $Ca^{2+}$ release channel could facilitate endo-lysosome interactions and lipid delivery to lysosomes. To our knowledge, these findings provide the first evidence indicating that NAADP-TRP-ML1 pathway plays a critical role in endocytic trafficking and, importantly, participates in lipid metabolism in lysosomes in these cells.

## GRANTS

This work is supported by National Heart, Lung, and Blood Institute Grants HL057244-09 and HL075316-0, and AD Williams Fund of the Virginia Commonwealth University.

## DISCLOSURES

No conflicts of interest, financial or otherwise, are declared by the author(s).

## REFERENCES

1. **Bargal R, Avidan N, Ben-Asher E, Olender Z, Zeigler M, Frumkin A, Raas-Rothschild A, Glusman G, Lancet D, Bach G.** Identification of the gene causing mucolipidosis type IV. *Nat Genet* 26: 118–123, 2000.
2. **Bargal R, Avidan N, Olender T, Ben Asher E, Zeigler M, Raas-Rothschild A, Frumkin A, Ben-Yoseph O, Friedlender Y, Lancet D, Bach G.** Mucolipidosis type IV: novel MCOLN1 mutations in Jewish and non-Jewish patients and the frequency of the disease in the Ashkenazi Jewish population. *Hum Mutat* 17: 397–402, 2001.
3. **Bargal R, Bach G.** Mucolipidosis type IV: abnormal transport of lipids to lysosomes. *J Inherit Metab Dis* 20: 625–632, 1997.
4. **Bassi MT, Manzoni M, Monti E, Pizzo MT, Ballabio A, Borsani G.** Cloning of the gene encoding a novel integral membrane protein, mucolipidin-and identification of the two major founder mutations causing mucolipidosis type IV. *Am J Hum Genet* 67: 1110–1120, 2000.
5. **Beck A, Kolisek M, Bagley LA, Fleig A, Penner R.** Nicotinic acid adenine dinucleotide phosphate and cyclic ADP-ribose regulate TRPM2 channels in T lymphocytes. *FASEB J* 20: 962–964, 2006.
6. **Bejarano I, Terron MP, Paredes SD, Barriga C, Rodriguez AB, Pariente JA.** Hydrogen peroxide increases the phagocytic function of human neutrophils by calcium mobilisation. *Mol Cell Biochem* 296: 77–84, 2007.
7. **Brailoiu E, Churamani D, Cai X, Schrlau MG, Brailoiu GC, Gao X, Hooper R, Boulware MJ, Dun NJ, Marchant JS, Patel S.** Essential requirement for two-pore channel 1 in NAADP-mediated calcium signaling. *J Cell Biol* 186: 201–209, 2009.
8. **Brailoiu E, Hooper R, Cai X, Brailoiu GC, Keebler MV, Dun NJ, Marchant JS, Patel S.** An ancestral deuterostome family of two-pore channels mediates nicotinic acid adenine dinucleotide phosphate-dependent calcium release from acidic organelles. *J Biol Chem* 285: 2897–2901, 2010.
9. **Bright NA, Gratian MJ, Luzio JP.** Endocytic delivery to lysosomes mediated by concurrent fusion and kissing events in living cells. *Curr Biol* 15: 360–365, 2005.
10. **Calcraft PJ, Ruas M, Pan Z, Cheng X, Arredouani A, Hao X, Tang J, Rietdorf K, Teboul L, Chuang KT, Lin P, Xiao R, Wang C, Zhu Y, Lin Y, Wyatt CN, Parrington J, Ma J, Evans AM, Galione A, Zhu MX.** NAADP mobilizes calcium from acidic organelles through two-pore channels. *Nature* 459: 596–600, 2009.
11. **Chen CS, Bach G, Pagano RE.** Abnormal transport along the lysosomal pathway in mucolipidosis, type IV disease. *Proc Natl Acad Sci U S A* 95: 6373–6378, 1998.
12. **Chen CS, Patterson MC, Wheatley CL, O'Brien JF, Pagano RE.** Broad screening test for sphingolipid-storage diseases. *Lancet* 354: 901–905, 1999.
13. **Christensen KA, Myers JT, Swanson JA.** pH-dependent regulation of lysosomal calcium in macrophages. *J Cell Sci* 115: 599–607, 2002.
14. **Churchill GC, Okada Y, Thomas JM, Genazzani AA, Patel S, Galione A.** NAADP mobilizes Ca(2+) from reserve granules, lysosome-related organelles, in sea urchin eggs. *Cell* 111: 703–708, 2002.
15. **Cole NB, Lippincott-Schwartz J.** Organization of organelles and membrane traffic by microtubules. *Curr Opin Cell Biol* 7: 55–64, 1995.
16. **Grynkiewicz G, Poenie M, Tsien RY.** A new generation of $Ca^{2+}$ indicators with greatly improved fluorescence properties. *J Biol Chem* 260: 3440–3450, 1985.
17. **Haller T, Dietl P, Deetjen P, Volkl H.** The lysosomal compartment as intracellular calcium store in MDCK cells: a possible involvement in InsP3-mediated $Ca^{2+}$ release. *Cell Calcium* 19: 157–165, 1996.
18. **Holroyd C, Kistner U, Annaert W, Jahn R.** Fusion of endosomes involved in synaptic vesicle recycling. *Mol Biol Cell* 10: 3035–3044, 1999.
19. **Huber LA, Fialka I, Paiha K, Hunziker W, Sacks DB, Bahler M, Way M, Gagescu R, Gruenberg J.** Both calmodulin and the unconventional myosin Myr4 regulate membrane trafficking along the recycling pathway of MDCK cells. *Traffic* 1: 494–503, 2000.
20. **Lange I, Penner R, Fleig A, Beck A.** Synergistic regulation of endogenous TRPM2 channels by adenine dinucleotides in primary human neutrophils. *Cell Calcium* 44: 604–615, 2008.
21. **Langhorst MF, Schwarzmann N, Guse AH.** $Ca^{2+}$ release via ryanodine receptors and $Ca^{2+}$ entry: major mechanisms in NAADP-mediated $Ca^{2+}$ signaling in T-lymphocytes. *Cell Signal* 16: 1283–1289, 2004.
22. **Lee HC, Aarhus R.** A derivative of NADP mobilizes calcium stores insensitive to inositol trisphosphate and cyclic ADP-ribose. *J Biol Chem* 270: 2152–2157, 1995.
23. **Li PL, Tang WX, Valdivia HH, Zou AP, Campbell WB.** cADP-ribose activates reconstituted ryanodine receptors from coronary arterial smooth muscle. *Am J Physiol Heart Circ Physiol* 280: H208–H215, 2001.
24. **Luzio JP, Poupon V, Lindsay MR, Mullock BM, Piper RC, Pryor PR.** Membrane dynamics and the biogenesis of lysosomes. *Mol Membr Biol* 20: 141–154, 2003.
25. **Moreschi I, Bruzzone S, Bodrato N, Usai C, Guida L, Nicholas RA, Kassack MU, Zocchi E, De Flora A.** NAADP+ is an agonist of the human P2Y11 purinergic receptor. *Cell Calcium* 43: 344–355, 2008.
26. **Mullock BM, Bright NA, Fearon CW, Gray SR, Luzio JP.** Fusion of lysosomes with late endosomes produces a hybrid organelle of intermediate density and is NSF dependent. *J Cell Biol* 140: 591–601, 1998.

26a. **Naylor E, Arredouani A, Vasudevan SR, Lewis AM, Parkesh R, Mizote A, Rosen D, Thomas JM, Izumi M, Ganesan A, Galione A, Churchill GC.** Identification of a chemical probe for NAADP by virtual screening. *Nat Chem Biol* 5: 220–226, 2009.

27. **Ohta S, Suzuki K, Tachibana K, Yamada G.** Microbubble-enhanced sonoporation: efficient gene transduction technique for chick embryos. *Genesis* 37: 91–101, 2003.
28. **Peters C, Mayer A.** $Ca^{2+}$/calmodulin signals the completion of docking and triggers a late step of vacuole fusion. *Nature* 396: 575–580, 1998.
29. **Pryor PR, Mullock BM, Bright NA, Gray SR, Luzio JP.** The role of intraorganellar Ca(2+) in late endosome-lysosome heterotypic fusion and in the reformation of lysosomes from hybrid organelles. *J Cell Biol* 149: 1053–1062, 2000.
30. **Pryor PR, Reimann F, Gribble FM, Luzio JP.** Mucolipin-1 is a lysosomal membrane protein required for intracellular lactosylceramide traffic. *Traffic* 7: 1388–1398, 2006.
31. **Slaugenhaupt SA, Acierno JS Jr, Helbling LA, Bove C, Goldin E, Bach G, Schiffmann R, Gusella JF.** Mapping of the mucolipidosis type IV gene to chromosome 19p and definition of founder haplotypes. *Am J Hum Genet* 65: 773–778, 1999.
32. **Steen M, Kirchberger T, Guse AH.** NAADP mobilizes calcium from the endoplasmic reticular Ca(2+) store in T-lymphocytes. *J Biol Chem* 282: 18864–18871, 2007.
33. **Storrie B, Desjardins M.** The biogenesis of lysosomes: is it a kiss and run, continuous fusion and fission process? *Bioessays* 18: 895–903, 1996.
34. **Sun M, Goldin E, Stahl S, Falardeau JL, Kennedy JC, Acierno JS Jr, Bove C, Kaneski CR, Nagle J, Bromley MC, Colman M, Schiffmann R, Slaugenhaupt SA.** Mucolipidosis type IV is caused by mutations in a gene encoding a novel transient receptor potential channel. *Hum Mol Genet* 9: 2471–2478, 2000.
35. **Taniyama Y, Tachibana K, Hiraoka K, Namba T, Yamasaki K, Hashiya N, Aoki M, Ogihara T, Yasufumi K, Morishita R.** Local delivery of plasmid DNA into rat carotid artery using ultrasound. *Circulation* 105: 1233–1239, 2002.
36. **Treusch S, Knuth S, Slaugenhaupt SA, Goldin E, Grant BD, Fares H.** Caenorhabditis elegans functional orthologue of human protein h-mucolipin-1 is required for lysosome biogenesis. *Proc Natl Acad Sci U S A* 101: 4483–4488, 2004.

37. **Vida T, Gerhardt B.** A cell-free assay allows reconstitution of Vps33p-dependent transport to the yeast vacuole/lysosome. *J Cell Biol* 146: 85–98, 1999.
38. **Yi FX, Zhang AY, Campbell WB, Zou AP, Van Breemen C, Li PL.** Simultaneous in situ monitoring of intracellular $Ca^{2+}$ and NO in endothelium of coronary arteries. *Am J Physiol Heart Circ Physiol* 283: H2725–H2732, 2002.
40. **Zhang F, Jin S, Yi F, Li PL.** TRP-ML1 functions as a lysosomal NAADP-sensitive Ca(2+) release channel in coronary arterial myocytes. *J Cell Mol Med* 13: 3174–3185, 2009.
41. **Zhang F, Li PL.** Reconstitution and characterization of a nicotinic acid adenine dinucleotide phosphate (NAADP)-sensitive $Ca^{2+}$ release channel from liver lysosomes of rats. *J Biol Chem* 282: 25259–25269, 2007.
42. **Zhang F, Xia M, Li PL.** Lysosome-dependent $Ca^{2+}$ release response to Fas activation in coronary arterial myocytes through NAADP: evidence from CD38 gene knockouts. *Am J Physiol Cell Physiol* 298: C1209–C1216, 2010.
43. **Zhang F, Zhang G, Zhang AY, Koeberl MJ, Wallander E, Li PL.** Production of NAADP and its role in $Ca^{2+}$ mobilization associated with lysosomes in coronary arterial myocytes. *Am J Physiol Heart Circ Physiol* 291: H274–H282, 2006.
44. **Zong X, Schieder M, Cuny H, Fenske S, Gruner C, Rotzer K, Griesbeck O, Harz H, Biel M, Wahl-Schott C.** The two-pore channel TPCN2 mediates NAADP-dependent Ca(2+)-release from lysosomal stores. *Pflügers Arch* 458: 891–899, 2009.